RAA 2021 Vol. 21 No. 11, 296(6pp) doi: 10.1088/1674-4527/21/11/296

*http://www.raa-journal.org* *http://iopscience.iop.org/raa*

*Research in Astronomy and Astrophysics*

# Method for differential phase delay resolution of phase referencing VLBI technique and its experimental verification

Huan Zhou[1], Jian-Guo Yan[1⋆], De-Zhen Xu[2], Yong Huang[3] and Hai-Tao Li[2]

[1] State Key Laboratory of Information Engineering in Surveying, Mapping and Remote Sensing, Wuhan University, Wuhan 430070, China; *jgyan@whu.edu.cn*

[2] Beijing Institute of Tracking and Telecommunications Technology, Beijing 100094, China

[3] Shanghai Astronomical Observatory, Chinese Academy of Science, Shanghai 200030, China

Received 2021 July 24; accepted 2021 August 23

**Abstract** The phase referencing Very Long Baseline Interferometry (VLBI) technique is a newly developed tool to measure the angular position of a deep space exploration probe in the plane-of-the-sky. Through alternating observations between the probe and a nearby reference radio source, their accurate relative angular separation can be obtained from the radio images generated by this technique. To meet the requirements of the current orbit determination software, differential delay should be firstly derived from those radio images. A method to resolve the differential phase delay from the phase referencing VLBI technique is proposed in this paper, and as well the mathematical model for differential phase ambiguity resolution is established. This method is verified with practical measurement data from the Chang'E-3 mission. The differential phase delay between the Chang'E-3 lander and rover was derived from the phase referencing VLBI measurements, and was then imported into the Shanghai astronomical observatory Orbit Determination Program (SODP) to calculate the position of the rover relative to the lander on the lunar surface. The results are consistent with those acquired directly from radio images, indicating that the differential phase ambiguity has been correctly resolved. The proposed method can be used to promote applications of the phase referencing VLBI technique in future lunar or deep space explorations, and more accurate orbit determination becomes promising.

**Key words:** Phase referencing VLBI technique — differential phase delay — radio interferometry — Chang'E-3 mission

## 1 INTRODUCTION

High-precision radio interferometry is an essential angular measurement technique for deep space exploration missions at this stage. The sensitivity of this technique to the motion of the spacecraft in the plane-of-the-sky can effectively complement traditional ground-based ranging and Doppler measurements, speed up the orbit determination process, and improve the orbit accuracy (Lanyi et al. 2007; Haitao et al. 2013). The observed results of radio interferometry techniques are time delay and delay rate of the spacecraft signal reaching the two remote stations. The spacecraft orbit determination software builds an observation model based on the measured geometric relationships, and then solves the spacecraft orbit by dynamical orbit determination theory (Yong 2006). Numerous deep spacecraft orbit determination software systems are available now. Some of them are well-known, such as the GEODYN II (Pavlis et al. 1998) developed by NASA Goddard Space Flight Center, Orbit Determination Program (ODP) (Panagiotacoupulos et al. 1846) developed by the U.S. Jet Propulsion Laboratory and GINS developed by CNES. There is some similar software developed in China including Beijing Aerospace Control Center Orbit Determination and Analysis Software (BODAS) software, Shanghai astronomical observatory Orbit Determination Program (SODP) software developed by the Shanghai Astronomical Observatory (Song-Jie & Ge-Shi 2010; Yong et al. 2009) and Wuhan University Deep space Orbit and Gravity System (WUDOGS) developed by Wuhan University. All of them support radio interferometry delay and delay rate observation data types. BODAS and SODP have successfully supported

⋆ Corresponding author

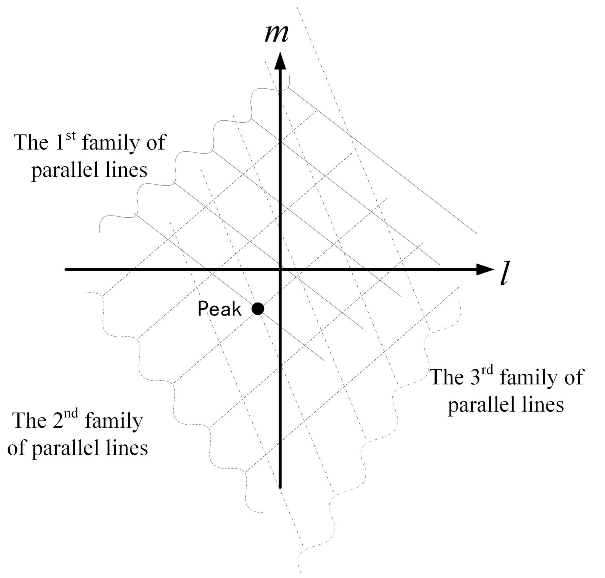


**Fig. 1** Different families of parallel lines generated by different $N$ and different $u, v$.

China's Chang'E series of exploration missions (Shi 2012; Huang et al. 2014), and WUDOGS has been successfully employed to solve the lunar gravity field using Chang'E orbital tracking data.

In order to improve the measurement accuracy, differential radio interferometry techniques are commonly applied in space exploration missions. By alternating observation of the spacecraft and the reference radio source, the observation of the reference radio signal can be utilized to correct the observation of the spacecraft signal and decrease the measurement errors introduced by the atmosphere, equipment and other factors. The observation thus obtained is also called differential time delay. Conventional differential radio interferometry techniques, such as delta-Very Long Baseline Interferometry (delta-VLBI) and delta-Differential One-way Ranging (delta-DOR) can be used to obtain the differential group delay. The accuracy of the measurements is limited by the bandwidth of the spacecraft downlink signal (Border et al. 2008; Curkendall & Border 2013; Rogers 1970).

The phase-referenced interferometry technique is a new type of radio interferometry technique that originates from radio astronomy interferometry (Thompson et al. 2008; Zensus et al. 1995). This technique achieves the interferometric phase difference between the radio source signal and the spacecraft signal by shortening the alternate observation period and decreasing the angular separation between the spacecraft and the reference source, and then directly obtains the right ascension (RA) and declination (Dec) difference between the spacecraft's prior angular position and the actual angular position through the phase referenced images (Lestrade et al. 1990). Zhou et al. conducted a preliminary study and test of this technique considering data from the Chang'E-3 mission to determine the position of the rover relative to the lander on the lunar surface (Zhou et al. 2015a,b). Since phase-referenced interferometry relies on differential phase, its measurement accuracy is consistent with differential phase delay and is much higher than differential group delay. However, the observations of this technique (i.e., the angular position deviation of the sky plane) are not compatible with the existing orbit determination software and cannot be used directly for spacecraft orbit determination, so it is necessary to study how to obtain the differential phase delay from the phase-referenced interferometry mapping.

This paper starts from the principle of spacecraft phase-referenced interferometry mapping and deduces a method for solving differential phase delay utilizing phase-referenced interferometry mapping results for the spacecraft point-source signal model. We carry out experimental verification of the method using the Chang'E-3 observation from the lander and the rover. With the acquired differential phase delay of the rover and lander, we successfully solve the relative positions of the two probes on the lunar surface employing the SODP orbit determination software. The accuracy is consistent with the positioning results of phase-referenced interferometry mapping. We arrange the paper in this way: In Section 2 we give the method to obtain differential phase time delay solution; The validation of this method by using the observation from the Chang'E-3 lander and rover is presented in Section 3; Finally, the conclusion is drawn in Section 4.

## 2 DIFFERENTIAL PHASE DELAY RESOLUTION METHOD

The traditional radio interferometry technique obtains the geometric transmission time delay difference of the source signal between two remote stations after correlation processing and fringe fitting. In contrast, the phase reference interferometry technique correlates the observed data from multiple measurement stations and obtains the angular position information of the target source directly through interferometry mapping. The basic principle of this technique is shown in the following equation.

$$\hat{I}(l,m) = \iint V(u,v,w)S(u,v)e^{2\pi i w}e^{2\pi i(ul+vm)}dudv, \tag{1}$$

where $\hat{I}(l,m)$ is the radio interferometric image of the spacecraft; $V(u,v,w)$ is the radio differential interferometry measurement. $V(u,v,w)$ is a complex number consisting of amplitude and phase, and the phase value

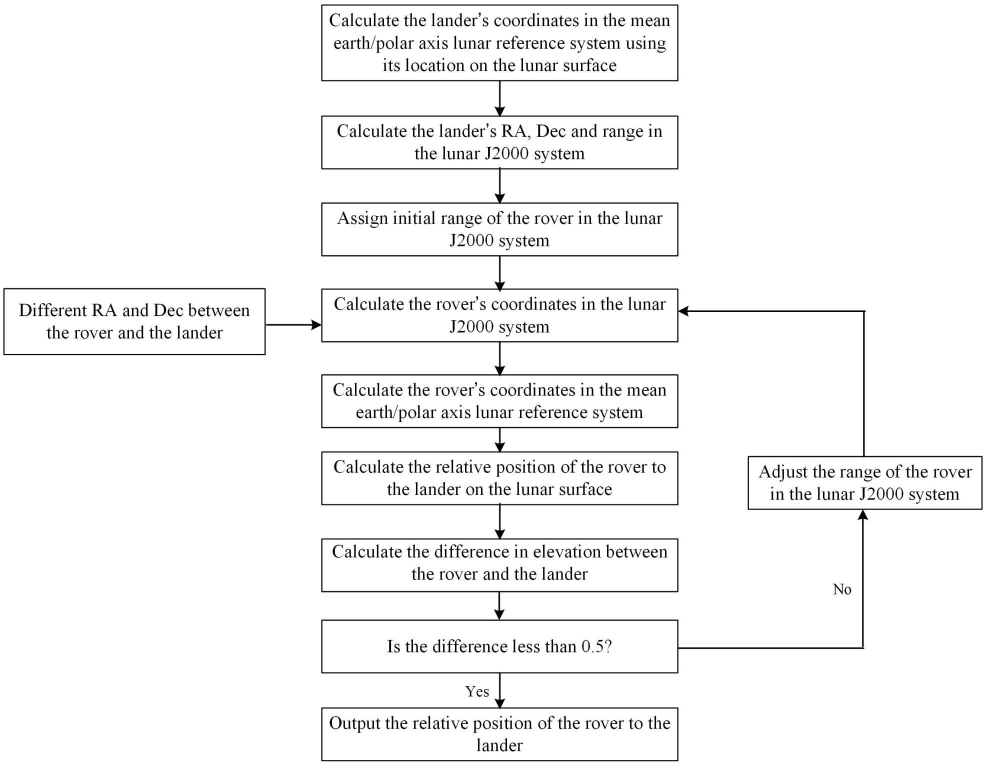


**Fig. 2** Flowchart of the method to calculate the relative positions of the rover and the lander on the lunar surface using their relative angular positions.

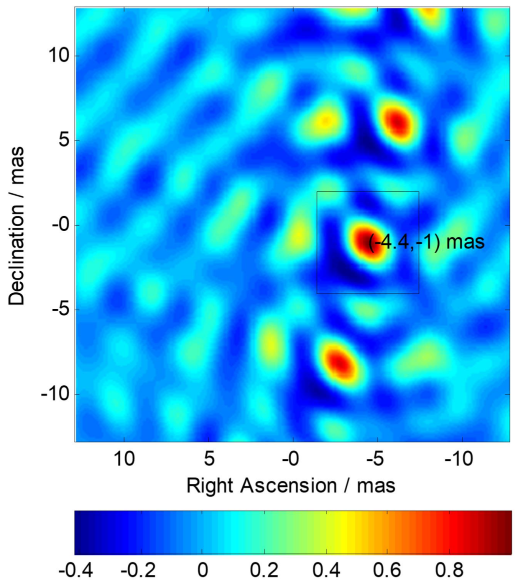


**Fig. 3** Phase referencing interferometry mapping of the rover.

is the differential phase resulting from the correlations between the target and reference source signal. $S(u,v)$ is the sampling function of all baselines in the $uv$ plane, i.e., the $uv$ coverage.

If we set the two-dimensional (2D) Fourier transform of $S(u,v)$ as $F(l,m)$ (also known as the dirty beam), then $\hat{I}(l,m)$ has a convolutional relationship with the real radio image $I(l,m)$ of the spacecraft as follows

$$\hat{I}(l,m) = I(l,m) \otimes F(l,m). \tag{2}$$

It is necessary to solve the above-mentioned convolution equation to obtain a real radio image of the spacecraft, which is a mathematically difficult problem. When the $uv$ coverage is poor, which means there are not enough stations or not enough observation time, the point spread function (PSF) of the dirty beam $F(l,m)$ will be poor. As a result, the quality of the image is greatly decreased and reliable radio images of the spacecraft cannot even be correctly obtained.

Assuming that the final radio interferometric image size is $M \times N$, the above convolution equation can be expressed as

$$\hat{I}(s,t) = \sum_{x=0}^{M-1} \sum_{y=0}^{N-1} I(x,y) F(s-x, t-y). \tag{3}$$

Treating the spacecraft as a point source with a normalized value, the real radio image of the spacecraft can be represented as a delta function

$$I(x,y) = \delta(x - \Delta l, y - \Delta m), \tag{4}$$

where $\Delta l$ and $\Delta m$ denote the offset of the spacecraft relative to the phase reference point (i.e., the image center).

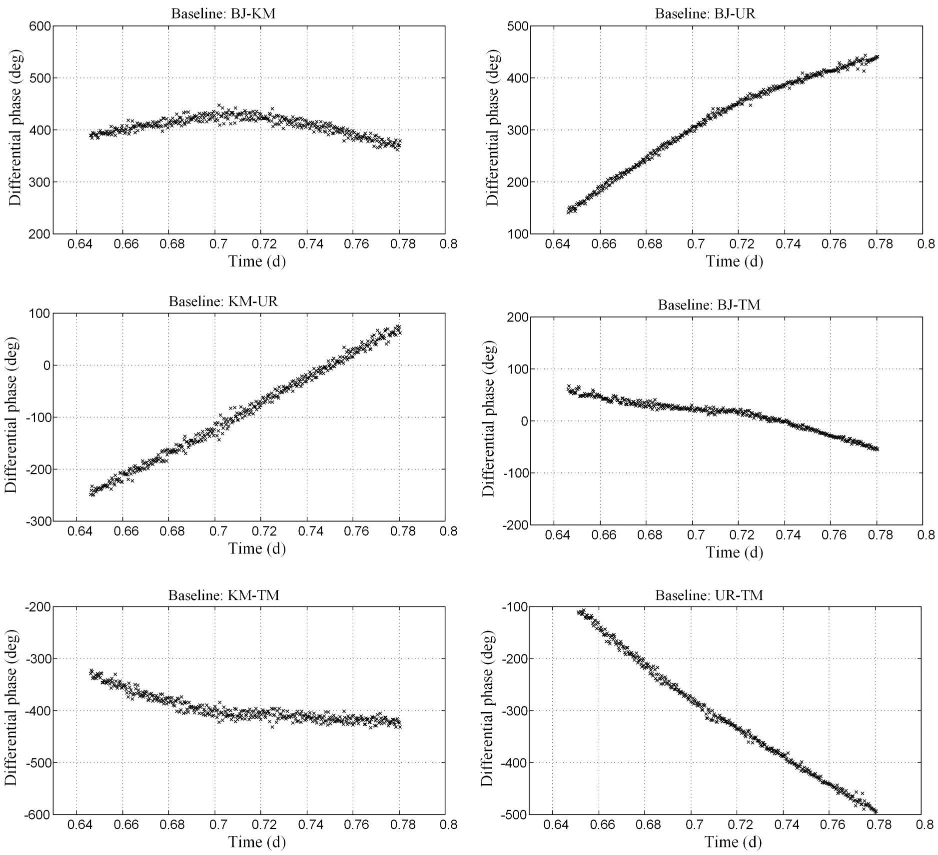


**Fig. 4** Differential phase of each baseline.

Thus, the convolution of Equation (3) can be reduced to

$$\hat{I}(s,t) = F(s-\Delta l, t-\Delta m). \tag{5}$$

Equation (5) demonstrates that the measured interferometric image of the spacecraft can be seen as the result of translation of the dirty beam. Because the dirty beam is a 2D Fourier transform of the $uv$ cover, i.e.,

$$F(s,t) = \iint S(u,v)e^{-2\pi i(us+vt)}dudv, \tag{6}$$

when the overlapping of samples is not considered, $S(u,v)$ can be seen as a sum of a series of delta functions.

$$S(u,v) = \sum_{i=1}^{M} \delta(u-u_i, v-v_i), \tag{7}$$

where $M$ is the number of sampling points in the $uv$ plane for all baselines during the observation time. Thus, the dirty beam can also be seen as a sum of a series of sinusoidal fringes, i.e.,

$$F(s,t) = \sum_{\substack{u_i=u_1,u_2,\ldots,u_M \\ v_i=v_1,v_2,\ldots,v_M}} \mathrm{Re}(e^{-2\pi i(u_i s+v_i t)}), \tag{8}$$

where $U$ and $V$ are the maximum range of horizontal and vertical coordinates of the $uv$ coverage respectively, and each sinusoidal fringe is the result of interferometric measurement per baseline. Thus, there are

$$\hat{I}(s,t) = \sum_{\substack{u_i=u_1,u_2,\ldots,u_M \\ v_i=v_1,v_2,\ldots,v_M}} \mathrm{Re}(e^{-2\pi i[u_i(s-\Delta l)+v_i(t-\Delta m)]}) \,. \tag{9}$$

So when $s = \Delta l$ and $t = \Delta m$, $\hat{I}(s,t)$ reaches its maximum value. Thus, the angular position offset of the spacecraft $\Delta l$ and $\Delta m$ can be obtained. The meaning of the offset is the difference between the a priori angular position and the actual angular position of the spacecraft and the reference source (Zhou et al. 2015b). If the reference source position is considered known and error-free, the offset directly reflects the difference between the spacecraft's a priori angular position and its actual angular position. Above is the principle of the phase-reference mapping method which uses the radio image to determine the angular position of the spacecraft.

Assuming that the differential interferometry measurements $V(u,v,w)e^{2\pi iw} = \mathrm{Re}^{(-\Delta\phi)}$, $R$ is the amplitude of the correlation, and $\Delta\phi$ is the differential phase of the spacecraft and reference source signals. With Equation (7) we can find

$$\hat{I}(s,t) = \sum_{\substack{u_i=u_1,u_2,\ldots,u_M \\ v_i=v_1,v_2,\ldots,v_M}} \mathrm{Re}(e^{-2\pi i(u_i s + v_i t - \Delta\phi_i/2\pi)}) \,. \tag{10}$$

So, when $\hat{I}(s,t)$ reaches the maximum value, we can arrive at the equation below from Equations (9) and (10)

$$u_i \Delta l + v_i \Delta m = \Delta\phi_i/2\pi \,. \tag{11}$$

Considering $\Delta\phi_i$ includes a phase integer cycle ambiguity, Equation (11) can be expressed as follows

$$\Delta\hat{\phi}_i = 2\pi(u_i \Delta l + v_i \Delta m) - 2N\pi, \tag{12}$$

where $\Delta\hat{\phi}_i \in (0, 2\pi]$ is the actual differential phase measurement obtained by radio interferometry and $N$ is the phase integer cycle ambiguity that needs to be resolved.

It can be seen that since the values of $\Delta l$ and $\Delta m$ are generally very small and usually vary negligibly with time over a period of hours (the spacecraft and radio source are very far away from the Earth), whereas the $u, v$ values vary significantly with time. Therefore, after obtaining $\Delta l$ and $\Delta m$ from the phase reference map, we can rely on Equation (12) to determine the differential phase integer cycle ambiguity for each baseline, and thus the exact differential phase delay of each baseline can be obtained.

The geometric explanation of the above process is as follows. From Equation (12) we can get

$$u\Delta l + v\Delta m = \Delta\phi/2\pi + N \,. \tag{13}$$

It follows that on the 2D plane established with $l$ and $m$ as coordinate axes, $\Delta l$ and $\Delta m$ must satisfy

$$\Delta l = (\Delta\phi/2\pi + N)/u - v\Delta m/u \,. \tag{14}$$

That means, in this plane, $\Delta l$ is linear with $\Delta m$, the direction of the line is $-v/u$, and the intersection with the coordinate axis is $(\Delta\phi/2\pi + N)/u$. If $N$ took different values, there will be a family of parallel lines in the plane. Furthermore, as we have different baselines with different orientations, we can get different $u, v$ values. It means we can obtain different families of lines, as illustrated in Figure 1. After superposition of all the lines, there will be a peak in the plane, which indicates the correct $\Delta l$ and $\Delta m$. Therefore, from the radio interferometric image, we find the location of the maximum value or the peak to obtain $\Delta l$ and $\Delta m$, and then the phase integer cycle ambiguity $N$ of each baseline can be determined from Equation (12).

## 3 CHANG'E-3 EXPERIMENTS

To verify the methods and models we proposed in Section 2, we undertook an experiment utilizing data from the Chang'E-3 mission. The Chang'E-3 mission consists of a lander and a rover, and the rover needs to be tracked and positioned during its lunar exploration (Sun et al. 2014). Due to the small angular distance between the lander and the rover in the plane-of-the-sky, both of them were visible at the same time in the main beam of the ground VLBI station. Therefore, the Chinese VLBI network conducted continuous same-beam mode observations of them, involving four radio telescopes, including Shanghai Tianma (TM, with a diameter of 65 m), Urumqi Nanshan (UR, with a diameter of 25 m), Yunnan Kunming (KM, with a diameter of 40 m) and Beijing Miyun (BJ, with a diameter of 40 m) (Wu et al. 2015).

In this experiment, we regarded the lander as the reference source and the rover as the target source to calculate their differential interferometry phase. Firstly, we obtained the phase referencing map of the rover employing the phase referencing VLBI technique. As both the rover and lander signal used the same time delay compensation model in the experiment, the phase referencing result of the rover directly reflects the RA and Dec relative to the lander. The data from the rover's onboard Guidance Navigation and Control (GNC) system indicated that the difference in elevation between the rover and the lander is less than 0.5 m around the landing area (Liu et al. 2015). Therefore, the relative angular position of the lander and rover in the plane-of-the-sky can be used to calculate the lunar surface position of the rover relative to the lander. The flowchart of this method is depicted in Figure 2.

Taking the observational data from 2013 December 20 as an example, when the rover was located not far from the lander, the phase referencing interferometry mapping results are displayed in Figure 3.

As shown in Figure 3, the RA and Dec difference between the rover and the lander is $(-4.4\pm0.2, -1.0\pm0.2)$ mas as determined from the image. After applying the method presented in Figure 2, we get the relative position of the rover to the lander with $(-3.36 \pm 0.4\text{N}, 8.44 \pm 0.4\text{E})$ m. According to Equation (12), the RA and Dec difference of the two instruments can be used to determine the phase integer cycle ambiguity of each baseline, which is displayed in Table 1.

In addition, we can obtain the differential phase of each baseline, as plotted in Figure 4.

Because the projection $(u_i, v_i)$ of the baseline in the $uv$ plane changed with time, from Figure 4 we can find that, during the observation interval, the differential phase of each baseline also varied with time. This is consistent with Equation (12). The differential phase can be further utilized to compute the differential phase delay following the simple relationship $\tau_p = (\Delta\hat{\phi}_i + 2N\pi)/2\pi f$, where $f$ is the signal frequency. We input the differential phase delay into the SODP orbit determination software, and find

**Table 1** Results of the Phase Integer Cycle Ambiguity of Each Baseline

| Baseline | BJ-KM | BJ-UR | BJ-TM | KM-UR | KM-TM | UR-TM |
|---|---|---|---|---|---|---|
| Phase integer cycle ambiguity | –1 | 0 | 0 | 1 | 1 | 0 |

**Table 2** Results of the Observation at Different Time Points

| Time point (BJT) | Relative positioning results Method in Fig. 2 | SODP |
|---|---|---|
| 2013-12-23 16:12:00 | $(-18.84 \pm 1.5\mathrm{N}, -0.79 \pm 0.7\mathrm{E})$ m | $(-16.45 \pm 1.5\mathrm{N}, -0.02 \pm 0.8\mathrm{E})$ m |
| 2013-12-24 00:30:00 | $(-25.45 \pm 1.5\mathrm{N}, 0.16 \pm 0.7\mathrm{E})$ m | $(-23.36 \pm 1.6\mathrm{N}, -0.15 \pm 0.9\mathrm{E})$ m |

the result of the rover to the lander is $(-3.69\pm0.5\mathrm{N}, 8.44\pm 0.5\mathrm{E})$ m. The accuracy of the two methods is about 1 m in each direction, and the difference between them is less than 0.5 m, which affirms that the differential phase delay generated by our method is correct and has high accuracy.

We also conducted similar processing using observational data of the two explorers at different time points. The results are listed in Table 2. The measurement error increases as the distance between the rover and lander grows due to the uncertainty in their elevation difference. However, it can still be seen that the differential phase delay generated by our method is correct and has high accuracy.

## 4 CONCLUSION

In this paper we propose a novel method to obtain the differential phase delay between the target spacecraft and the reference source from the phase-referenced interferometry mapping results. In theory, it works not only for the in-beam observation, but also the out-of-beam observation. We also realize the conversion from the relative angular position measurements to high-accuracy differential phase delay measurements, and effectively adapt them to the SODP orbit determination software. The validity and correctness of the method are verified through the observational data of the lander and rover in the Chang'E-3 mission. This work lays a solid foundation for the next engineering application of phase-referenced interferometry technology in future China deep space exploration missions, including Zhurong rover positioning in China's first Mars mission "Tianwen-1". We are now trying to conduct out-of-beam VLBI phase referencing observation of the "Tianwen-1" orbiter around Mars using the VLBI network in China. A radio source will be chosen as the reference source, and position of the orbiter will be determined relative to the radio source.

**Acknowledgements** The authors thank the Shanghai Astronomical Observatory, Chinese Academy of Sciences, for processing and formatting the interferometric data from the Chang'E-3 mission. The work is supported by the National Natural Science Foundation of China (Grant Nos. 42030110, 61603008 and U1831132) and the Innovation Group of Natural Fund of Hubei Province (2018CFA087).

## References

Border, J. S., Lanyi, G. E., & Shin, D. K. 2008, Radiometric Tracking for Deep Space Navigation (AAS 08-052), in Proceedings of the 31st annual AAS Rocky Mountain Guidance and Control Conference, 131, 309

Curkendall, D. W., & Border, J. S. 2013, in Interplanetary Network Progress Report, 42, 1

Fomalont, E. 2005, Charlottesville, Virginia: NRAO Memorandum,

Haitao, L., Huan, Z., & Wanhong, H. 2013, Journal of Flight Vehicle Measurement and Control, 32, 470

Yong, H. 2006, Ph. D. Dissertation

Huang, Y., He, X., & Cao, J. 2014, Science Bulletin, 59, 2268

Lanyi, G. E., Bagri, D. S., & Border, J. S. 2007, IEEE Proceedings, 95, 2193

Lestrade, J., Rogers, A., Whitney, A. R., et al. 1990, AJ, 99, 1663

Liu, Z. Q., Di, K. C., & Peng, M. 2015, Science China Physics Mechanics & Astronomy, 58, 019601

Panagiotacoupulos, N. D., Zielenbach, J. W., & Duesing, R. W. 1846, NASA Technical Report 37, 1974

Pavlis, D. E., Luo, S., & Dahiroc, P. 1998, NASA GSFC,

Rogers, A. E. 1970, Radio Science, 5, 1239

Shi, T. G. 2012, Beijing: National Defense Industry Press,

Song-Jie, H., & Ge-Shi, T. 2010, Journal of Flight Vehicle Measurement and Control, 29, 69

Sun, Z., Zhang, T., Zhang, H., et al. 2014, Science in China: Technology Science, 44, 331 (in Chinese)

Thompson, A. R., Moran, J. M., & Swenson, J. G. W. 2008, Interferometry and Synthesis in Radio Astronomy (New Jersey: John Wiley & Sons)

Wu, W., Liu, Q., Huang, Y., et al. 2015, Journal of Deep Space Exploration, 2, 34 (in Chinese)

Yong, H., Xiaogong, H., & Jianfeng, C. 2009, Journal of Flight Vehicle Measurement and Control, 28, 83

Zensus, J. A., Diamond, P. J., Napier, P. J. 1995, Very Long Baseline Interferometry and the VLBA, ASPC Series, 82

Zhou, H., Li, H. T., & Dong, G. L. 2015a, Science China: Information Sciences, 58, 092201

Zhou, H., Tong, F., Li, H., et al. 2015b, Acta Geodaetica et Cartographica Sinica, 44, 634 (in Chinese)